

# SWB I-Shaped Microstrip Patch Antenna with Extended Ground Plane Structure for 5G and beyond 5G Applications

Sanaa Iriqat

Department of Electronic and Communication Engineering, Al-Quds University, Jerusalem, Palestine  
sanairiqat.94@gmail.com (corresponding author)

Received: 18 September 2024 | Revised: 21 October 2024 | Accepted: 29 October 2024

Licensed under a CC-BY 4.0 license | Copyright (c) by the authors | DOI: <https://doi.org/10.48084/etasr.9036>

## ABSTRACT

This study presents an I-shaped antenna with an extended ground plane structure, which plays a pivotal role in markedly enhancing the antenna's performance in terms of bandwidth, gain, and efficiency across a multitude of 5G mm-wave bands, including 28 GHz, 39 GHz, 41 GHz, 60 GHz, 73 GHz, and others. The proposed antenna exhibits Super Wideband (SWB) characteristics, with a frequency range extending from 25.5 GHz to beyond. It also demonstrates a peak gain of 10.75 dBi and a maximum radiation efficiency of 88%. The compact dimensions of the design, measuring  $7 \times 10.6 \times 1.52$  mm<sup>3</sup>, facilitate the attainment of high gain (10.75 dBi), SWB characteristics (25.5–80 GHz), and high radiation efficiency (<88%), rendering it a promising contender for prospective 5G and B5G applications.

**Keywords-**patch antenna; 5G; B5G; Super Wideband (SWB); extended ground plane

## I. INTRODUCTION

It is anticipated that Fifth Generation (5G) and Beyond 5G (B5G) technology will satisfy the requirements for higher data rates and lower latency [1]. The evolution of applications such as the Internet of Things (IoT) [2], smart energy [3], augmented and virtual reality [4], and driverless cars [5], among others, forces antenna engineers to design antennas capable of covering a wide range of frequencies with well-defined radiation characteristics. This is due to the fact that each application may operate in a different frequency range with distinct radiation characteristics. Microstrip patch antennas are of significant importance in wireless communication systems, including 5G, due to their distinctive advantages and inherent limitations. One of their primary advantages is their compact and low-profile structure, which renders them highly suitable for integration into modern communication devices, including smartphones, base stations, and wearable technology [6]. This compactness is of critical importance for 5G, where dense networks comprising multiple antenna arrays are deployed in order to meet the high capacity and coverage demands. Furthermore, their planar configuration permits straightforward integration into conformal or embedded designs, which is a crucial consideration for prospective 5G applications that necessitate seamless and inconspicuous antenna installation [7]. However, microstrip patch antennas also encounter notable challenges in 5G applications. One significant disadvantage is their inherently narrow bandwidth, which constrains their capacity to support the Ultra-Wideband (UWB) requirements of 5G mm-wave frequencies. Techniques such as superstrate, stacked patches, and meta-surfaces are often employed to extend the bandwidth, but these solutions can introduce

complexity and increase design constraints [8]. A further disadvantage is their relatively low radiation efficiency, particularly at higher frequencies, where surface wave losses and dielectric losses become more pronounced. This has the potential to impact the overall system performance in high-frequency 5G applications.

The 5G spectrum is divided into two categories: sub-6 GHz/sub-7 GHz and mm-wave [9]. While frequencies below 6 GHz and below 7 GHz offer broader coverage and penetration, the mm-wave spectrum is ideal for delivering high data rates over shorter distances, making it particularly suited for dense urban environments [10]. The mm-wave spectrum encompasses a range of frequency bands, including the 28 GHz band (26.5–29.5 GHz), the 39 GHz band (37–40 GHz), the 41 GHz band (39.5–43.5 GHz), the 60 GHz band (57–64 GHz), and others [11, 12]. The literature contains numerous discussions of antenna designs for mm-wave applications. For example, authors in [13] introduce a slotted patch antenna with wideband characteristics for 28 GHz 5G applications. The antenna exhibits an impedance bandwidth of 4.841 GHz (24.356–29.197 GHz) and a peak gain of 8.54 dBi. The dimensions of the proposed antenna are  $30 \times 40$  mm<sup>2</sup>. Authors in [14], present a circularly polarized patch antenna for 28 GHz applications. To achieve impedance matching, a tapered feed line is utilized, resulting in an impedance bandwidth of approximately 1 GHz (27.5 – 28.5 GHz). The presented patch antenna offers a maximum gain of 7.3 dBi. Authors in [15], proposed a line-structured patch antenna with a slotted ground plane as a potential solution for 5G mm-wave applications. The antenna exhibits a wide bandwidth of 4.846 GHz (26.154 - 31 GHz) with overall dimensions of  $20 \times 20$  mm<sup>2</sup>. Authors in [16],

outlined a monopole antenna design for 38 GHz mm-wave applications. The presented antenna exhibits a resonant frequency of 38 GHz and provides a bandwidth of 3 GHz (36.6–39.6 GHz) through the incorporation of a rectangular slot in the circular patch. The dimensions of the single antenna are 12 mm by 12 mm. Authors in [17], showed a dual-band monopole antenna designed for 28 GHz and 38 GHz applications, employing a double stub matching technique. The antenna has dimensions of  $8 \times 7 \text{ mm}^2$  and attains a maximum gain of 7 dBi. The impedance bandwidth of the antenna is 1.75 GHz (27–28.75 GHz) and 6.23 GHz (36.20–42.43 GHz). Authors in [18], designed a dual-band microstrip patch antenna for 28 GHz and 38 GHz mm-wave applications. The antenna comprises two radiating patches, namely a main patch and a parasitic patch. The impedance bandwidth is 0.6 GHz in both frequency ranges, specifically 27.7–28.3 GHz and 37.7–38.3 GHz, and the maximum gain is 8.1 dBi. Authors in [19], proposed a dual-band (38/60 GHz) patch antenna with a Defected Ground Structure (DGS), for use in 5G wireless applications. The antenna incorporates a semicircular notched patch in conjunction with two circular etched patches, which are positioned and dimensioned in a strategic manner to achieve optimal performance. The impedance bandwidth is 700 MHz at 38 GHz and 1 GHz at 60 GHz. The antenna attains a peak gain of 6.2 dBi and incorporates a partial ground plane with dimensions of  $25 \times 23 \text{ mm}^2$ . Authors in [20], presented a compact antenna design for 5G millimeter-wave applications. The proposed antenna incorporates a circular patch with a circular slot at one of its corners, while the ground plane comprises a mesh-like structure in conjunction with four circular parasitic elements. The antenna offers a bandwidth of 17.6 GHz for UWB operations, spanning a frequency range from 16.2 to 33.8 GHz. Additionally, the antenna attains a peak gain of 3.85 dBi and exhibits dimensions of  $12 \times 14 \text{ mm}^2$ . Authors in [21], presented a surface-waveband (SWB) monopole antenna. The half-elliptical printed monopole is designed with a triangular inset added to the ground plane, along with bent edges, with the objective of enhancing the antenna's bandwidth. The proposed monopole antenna exhibits characteristics of both sub-6 GHz and mm-wave bands, starting at 0.5 GHz and exhibiting characteristics of a SWB antenna. Nevertheless, the antenna achieves a peak gain of 11.2 dBi and has relatively large dimensions of  $200 \times 220 \text{ mm}^2$ . Authors in [22], showed a SWB monopole antenna. The antenna exhibits a notable bandwidth of 25.25 GHz (2.75–28 GHz) and a realized gain of 4.80 dBi. The radiating patch is based on a modified rectangular design, incorporating a stepwise matching structure to enhance performance. The overall dimensions of the antenna are  $26 \times 26 \text{ mm}^2$ . Authors in [23], developed a compact antenna composed entirely of textile materials with SWB characteristics, for applications in radio frequency energy harvesting and wearable technology. The antenna exhibits a broad frequency range, spanning from 3.16 to 50 GHz, and attains a peak gain of 7.70 dBi at 23.05 GHz.

The extended ground plane structure has been proven effective in enhancing the performance of microstrip patch antennas at 60 GHz, particularly in terms of bandwidth and radiation efficiency, as discussed by authors in [24]. In this study, the extended ground plane structure technique is

employed with the objective of improving antenna performance not only for the 60 GHz band but also for the majority of mm-wave bands that have been assigned for use in 5G applications. The employment of an I-shaped antenna design with an extended ground plane enables the realization of a SWB commencing at 25.5 GHz, encompassing licensed and unlicensed 5G mm-wave bands such as 28 GHz, 39 GHz, 41 GHz, 60 GHz, 73 GHz, and others. The antenna attains a peak gain of 10.75 dBi and a maximum radiation efficiency of 88%. The proposed design is notably compact, measuring only  $7 \times 10.6 \times 1.52 \text{ mm}^3$ , yet it offers high gain, high radiation efficiency, and SWB behavior, making it a compelling alternative to other mm-wave patch antenna designs.

## II. ANTENNA THEORY AND DESIGN

### A. I-Shaped Patch Antenna Design

The proposed antenna is based on a rectangular patch with an extended ground plane structure, as presented in Figure 1. A quarter-wavelength transformer with a characteristic impedance of  $75 \Omega$  is employed to match the rectangular patch to a  $50 \Omega$  microstrip line.

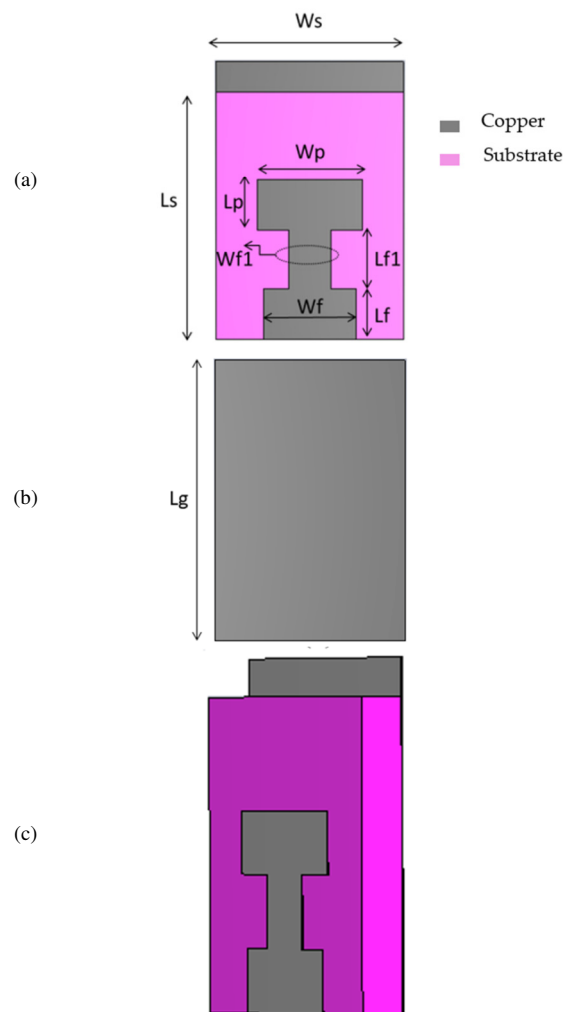


Fig. 1. Antenna design structure (a) front, (b) back, (c) 3D view.

TABLE I. FINAL DIMENSIONAL PARAMETERS OF THE PROPOSED ANTENNA

Parameter	Dimension (mm)	Parameter	Dimension (mm)
$W_s$	7	$L_p$	2
$W_p$	4	$L_f$	1.9
$W_f$	3.5	$L_{fl}$	2.2
$W_{fl}$	1.6	$L_g$	10.6
$L_p$	9.3		

B. Analysis of the Extended Ground Plane Structure

The extended ground plane structure is of critical importance in determining the behavior of the proposed antenna. Figure 2 presents the antenna designs with and without a ground plane structure, while Figure 3 shows the antenna's performance with and without the extended ground plane structure, displaying the corresponding reflection coefficient, gain, and radiation efficiency for both configurations.

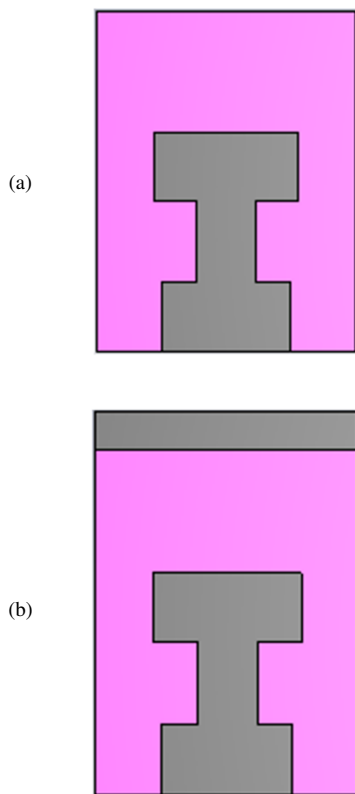


Fig. 2. Antenna design structure (a) with extended ground plane (b) without extended ground plane.

The extended ground plane structure facilitates enhanced impedance matching, thereby enabling SWB behavior to commence at 25.5 GHz and encompass the designated bands for 5G mm-wave applications. Moreover, the extended ground plane structure enhances gain, particularly in the upper mm-wave spectrum. This structure enables a more efficient radiation mechanism at higher frequencies by reducing losses and optimizing energy radiation in higher bands, where such

performance is typically more challenging to achieve due to increased losses. Furthermore, the extended ground plane improves radiation efficiency not only at high frequencies but across most of the frequency range (Figure 3(c)). It also plays a role in reducing undesired radiation modes, enhancing the directional radiation pattern of the antenna, which helps focus its energy more effectively, leading to increased gain and efficiency.

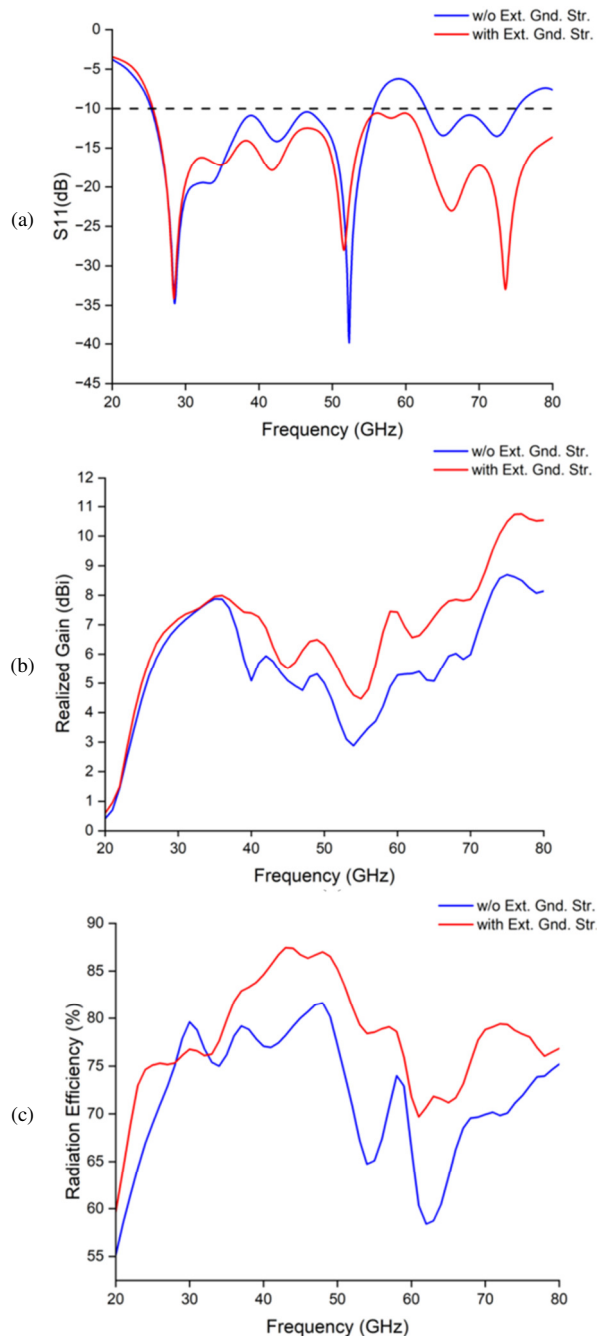


Fig. 3. Antenna design with and without extended ground plane structure (a) reflection coefficient (b) realized gain (c) radiation efficiency.

C. Parametric Analysis

The principal objective of this study is to develop a compact patch antenna with SWB capabilities that can accommodate a range of mm-wave communication bands, thereby addressing both current and future requirements for 5G and beyond. To this end, an extensive parametric analysis was conducted for each parameter. This section presents some of the study's most significant findings. The length of the patch,  $L_p$ , is a critical parameter that significantly influences the bandwidth of the antenna. As shown in Figure 4(a), the length of the patch ( $L_p$ ) was varied between 1.5 and 4 mm. The optimal bandwidth was achieved at  $L_p = 2$  mm, which aligns with the theoretical value calculated using (2) for a resonance frequency of 28 GHz. Furthermore, the length of the quarter-wave transformer ( $L_{f1}$ ) was examined, as presented in Figure 4(b). This parameter was varied between 1.2 and 4.2 mm. The optimal impedance matching was observed when  $L_{f1} = 2.2$  mm, which is approximately equals to  $\lambda_o/4$  at 28 GHz.

III. RESULTS AND DISCUSSION

A. Reflection Coefficient

Figure 5 presents the S11 parameter plot, which indicates that the proposed antenna exhibits SWB behavior across the frequency range of 25.5 GHz to 80 GHz. Four prominent notches are evident at 28.3 GHz, 51.5 GHz, 66.5 GHz, and 73.5 GHz, which represent key resonant frequencies.

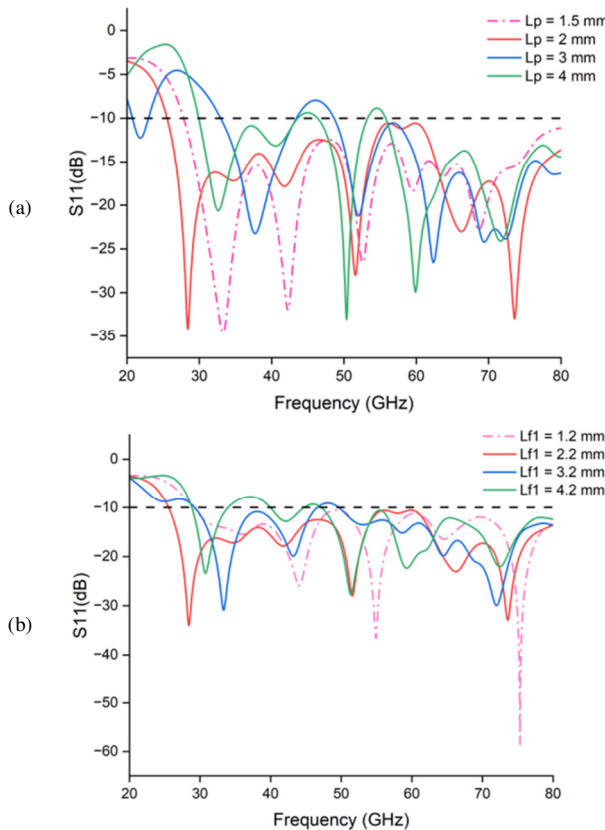


Fig. 4. Reflection coefficient variation with different values of (a)  $L_p$  (b)  $L_{f1}$ .

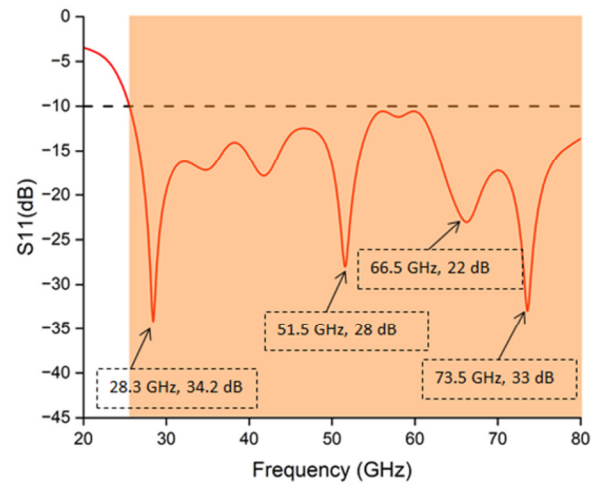


Fig. 5. Simulated results for the reflection coefficient of the designed antenna.

The observed notches correspond to frequencies where the reflection coefficient exhibits a notable decline below the -10 dB threshold, indicating optimal impedance matching and minimal signal reflection at those points.

The extensive frequency range encompassed by the SWB antenna, in conjunction with the precise notch characteristics, indicates that the antenna is capable of effective operation across a multitude of mm-wave communication bands, rendering it an optimal choice for 5G and prospective high-frequency applications.

B. Realized Gain and Radiation Efficiency

Figure 6 shows the realized gain and radiation efficiency of the antenna, which exhibits a peak gain of 10.75 dBi at elevated frequencies. This indicates a notable degree of directivity and concentrated radiation within this frequency range. Furthermore, the antenna demonstrates a high level of radiation efficiency, reaching a maximum of 88%. This makes the antenna highly efficient, particularly within the 25.5 to 58 GHz range.

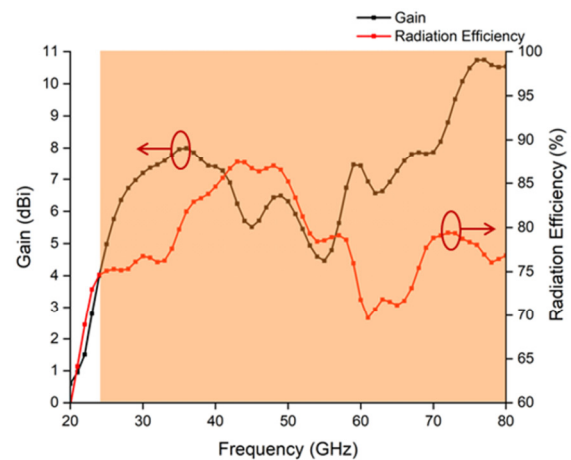


Fig. 6. Simulated results for the gain and radiation efficiency of the designed antenna.

C. Radiation Patterns

Figure 7 presents the three-dimensional (3D) radiation patterns of the antenna at frequencies of 28 GHz and 39 GHz. As shown in Figures 7(a) and 7(b), the 3D radiation patterns exhibit directional characteristics at both frequencies, which can be attributed to the high gain achieved. The two-dimensional (2D) radiation patterns for both frequencies are presented in Figures 8(a) and 8(b), respectively. At 28 GHz, the maximum radiation occurs at an angle of  $14^\circ$  in the *E*-plane, while in the *H*-plane, the main lobe is directed at an angle of  $0^\circ$ . In contrast, at 39 GHz, the main lobe of the radiation pattern is directed at  $\theta = 27^\circ$  in the *E*-plane and  $\theta = 0^\circ$  in the *H*-plane.

IV. COMPARISON OF THE PROPOSED SWB ANTENNA WITH THE LITERATURE

Table II presents a comparison of the performance of the designed antenna with that of previously published works in the existing literature. The antenna designs discussed in [12-18] are oriented towards the 28 GHz, 39 GHz, or 60 GHz bands, yet they exhibit limited bandwidth. In contrast, authors in [19-21] presented antenna designs with wideband and SWB characteristics, though this is accompanied by an increase in the dimensions of the antenna. The presented design exhibits SWB characteristics, covering a broad range of mm-wave bands, including 28 GHz, 39 GHz, 41 GHz, 60 GHz, and 73 GHz.

The implementation of an extended ground plane structure is of significant importance in the enhancement of impedance matching across a wide range of frequencies. This technique enhances the antenna's ability to support multiple resonances, thereby facilitating wideband and SWB performance. Moreover, the selection of the substrate material, Rogers RO4003C, with a relatively thicker substrate thickness of 1.52 mm, enables more precise control of the effective dielectric constant and reduction of surface wave losses, resulting in enhancements in both radiation efficiency and bandwidth. In contrast, designs using thinner substrates, such as RT5880, presented by authors in [15, 17], exhibit reduced bandwidth. The proposed antenna achieves a high peak gain of 10.75 dBi, which makes it a strong candidate for applications related to the fifth generation of mobile technology and beyond.

V. CONCLUSIONS

This study proposes a Super Wideband (SWB) I-shaped patch antenna for use in 5G and B5G mm-wave applications. The innovation of this research lies in the effective usage of the extended ground plane structure, which enables the antenna to achieve multiple resonance points and operate across a broader range of mm-wave sub-bands, from 25.5 GHz to 80 GHz. This enhances the antenna's versatility and performance in high-data-rate communication systems.

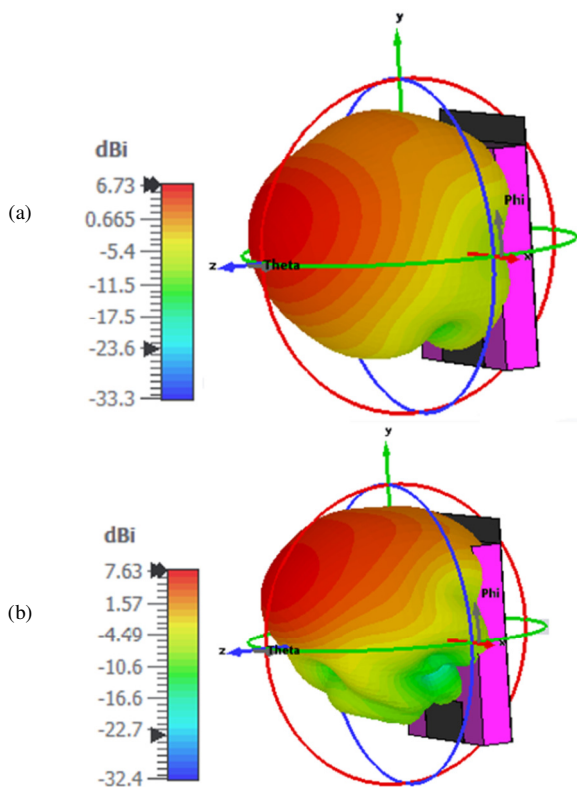


Fig. 7. 3D radiation patterns at (a) 28 GHz (b) 39 GHz.

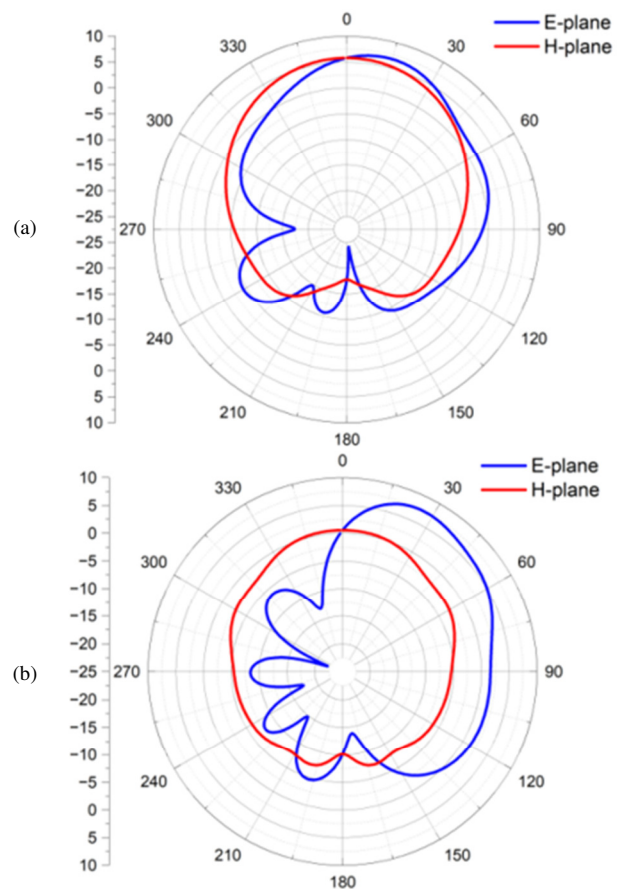


Fig. 8. 2D radiation patterns at (a) 28 GHz (b) 39 GHz.

TABLE II. COMPARISON OF PRESENTED SWB ANTENNA WITH PREVIOUS WORKS

Ref.	Bandwidth (GHz)	Antenna Dimensions d(mm <sup>2</sup> )	Substrate material	Peak gain (dBi)
[13]	24.356 – 29.197	30 × 40	RT5858 (h =1.575 mm)	8.54
[14]	27.5 – 28.5	NA	RO3003 (h =0.25 mm)	7.3
[15]	26.154 - 31	20 × 20	RT5880 (h =0.79 mm)	5.22
[16]	36.6 - 39.6	12 × 12	RT4003 (h =0.203 mm)	NA
[17]	27–28.75, 36.20–42.43	8 × 7	RT5880 (h =0.254 mm)	7
[18]	27.7–28.3, 37.7–38.3	8 × 18	RO3003 (h =0.25 mm)	8.1
[19]	38–38.7, 59.5–60.5	NA	RO4003 (h =0.203 mm)	6.2
[20]	16.2–33.8	12 × 14	FR4 (h =1.6 mm)	3.85
[21]	0.5 – 40	200 × 220	TLY-5 (h = 1.57 mm)	11.2
[22]	2.75–28	26 × 26	FR4 (h =1.6 mm)	4.80
[23]	3.16 – 50	30 × 25	Felt (h = 1 mm)	7.70
Proposed antenna	25.5–80	7 × 10.6	RO4003C (h =1.52 mm)	10.75

In comparison to previously published works, the proposed design exhibits superior performance in terms of frequency coverage, gain (10.75 dBi), and radiation efficiency (<88%) in a more compact form factor. Consequently, it is a highly competitive candidate for mm-wave applications. However, minor fluctuations in both gain and radiation efficiency have been observed at certain frequencies. Future work will concentrate on optimizing these characteristics to guarantee more consistent performance across the entire bandwidth while maintaining the wideband and high-gain attributes. Moreover, the single antenna design will be further developed into a Multiple-Input, Multiple-Output (MIMO) configuration with the objective of enhancing diversity and throughput in multi-user environments. Furthermore, experimental validation will be conducted through measurements in real-world scenarios to assess the robustness of the design in 5G and B5G systems. This will include testing in both indoor and outdoor environments to account for the different propagation conditions that may be encountered.

## REFERENCES

- [1] U. Ghafoor, M. Ali, H. Z. Khan, A. M. Siddiqui, and M. Naeem, "NOMA and future 5G & B5G wireless networks: A paradigm," *Journal of Network and Computer Applications*, vol. 204, Aug. 2022, Art. no. 103413, <https://doi.org/10.1016/j.jnca.2022.103413>.
- [2] K. Elgazzar *et al.*, "Revisiting the internet of things: New trends, opportunities and grand challenges," *Frontiers in the Internet of Things*, vol. 1, Nov. 2022, <https://doi.org/10.3389/friot.2022.1073780>.
- [3] J. Em-Udom and N. Jaisumroum, "SDT Smart Hybrid Streetlight Pole Design Utilizing Renewable Energy for a Smart City in Thailand," *Smart Grids and Sustainable Energy*, vol. 8, no. 3, Oct. 2023, Art. no. 16, <https://doi.org/10.1007/s40866-023-00173-2>.
- [4] A. M. Al-Ansi, M. Jaboob, A. Garad, and A. Al-Ansi, "Analyzing augmented reality (AR) and virtual reality (VR) recent development in education," *Social Sciences & Humanities Open*, vol. 8, no. 1, Jan. 2023, Art. no. 100532, <https://doi.org/10.1016/j.ssaho.2023.100532>.
- [5] S. Agriesti *et al.*, "Impact of Driverless Vehicles on Urban Environment and Future Mobility," *Transportation Research Procedia*, vol. 49, pp. 44–59, Jan. 2020, <https://doi.org/10.1016/j.trpro.2020.09.005>.
- [6] A. Khan, A. Ahmad, and M. Alam, "A High-Gain Reflector- DGS-Superstates -Enabled Quad-Band 5G-Antenna for mm-wave Applications," *Transactions on Electromagnetic Spectrum*, vol. 3, no. 1, pp. 34–50, 2024, <https://doi.org/10.5281/zenodo.8363039>.
- [7] P. Gupta and V. Gupta, "Linear 1 × 4 Microstrip Antenna Array Using Slotted Circular Patch for 5G Communication Applications," *Wireless Personal Communications*, vol. 127, no. 4, pp. 2709–2725, Dec. 2022, <https://doi.org/10.1007/s11277-022-09896-4>.
- [8] N. Hussain, M.-J. Jeong, A. Abbas, and N. Kim, "Metasurface-Based Single-Layer Wideband Circularly Polarized MIMO Antenna for 5G Millimeter-Wave Systems," *IEEE Access*, vol. 8, pp. 130293–130304, 2020, <https://doi.org/10.1109/ACCESS.2020.3009380>.
- [9] S. Iriqat, S. Yenikaya, and M. Secmen, "Dual-Band 2 × 1 Monopole Antenna Array and Its MIMO Configuration for WiMAX, Sub-6 GHz, and Sub-7 GHz Applications," *Electronics*, vol. 13, no. 8, Jan. 2024, Art. no. 1502, <https://doi.org/10.3390/electronics13081502>.
- [10] B. A. Hussein, "Millimeter Waves for 5G and Beyond in Smart IOT Applications," M.S. thesis, Near East University, Nicosia, Cyprus, 2021.
- [11] *Global 5G spectrum update and innovations for future wireless systems*. San Diego, CA, USA: Qualcomm, 2023.
- [12] I. O. Babarinde, J. S. Ojo, and M. O. Ajewole, "High-Capacity Millimeter Wave Channel for 5G and Future Generation Systems Deployment in Tropical Region using NYUSIM Algorithm," *Transactions on Electromagnetic Spectrum*, vol. 3, no. 1, pp. 1–19, 2024, <https://doi.org/10.5281/zenodo.8269340>.
- [13] L. C. Paul and H. K. Saha, "A Wideband Microstrip Line Feed Slotted Patch Antenna for 28 GHz 5G Applications," in *2021 International Conference on Electronics, Communications and Information Technology (ICECIT)*, Khulna, Bangladesh, Sep. 2021, <https://doi.org/10.1109/ICECIT54077.2021.9641230>.
- [14] M. Abo. El-Hassan, A. E. Farahat, and Khalid. F. A. Hussein, "Circularly Polarized 28 GHz Compact Patch Antenna for 5G Mobile Communications," in *2021 International Telecommunications Conference (ITC-Egypt)*, Alexandria, Egypt, Jul. 2021, pp. 1–6, <https://doi.org/10.1109/ITC-Egypt52936.2021.9513891>.
- [15] L. C. Paul, S. C. Das, N. Sarker, R. Azim, Md. F. Ishraque, and Sk. A. Shezan, "A Wideband Microstrip Patch Antenna with Slotted Ground Plane for 5G Application," in *2021 International Conference on Science & Contemporary Technologies (ICSCCT)*, Dhaka, Bangladesh, Aug. 2021, pp. 1–5, <https://doi.org/10.1109/ICSCCT53883.2021.9642597>.
- [16] A. A. Ibrahim, W. A. E. Ali, M. Alathbah, and A. R. Sabek, "Four-Port 38 GHz MIMO Antenna with High Gain and Isolation for 5G Wireless Networks," *Sensors*, vol. 23, no. 7, Jan. 2023, Art. no. 3557, <https://doi.org/10.3390/s23073557>.
- [17] P. S. Bhadravathi Ghouse *et al.*, "Dual-Band Antenna at 28 and 38 GHz Using Internal Stubs and Slot Perturbations," *Technologies*, vol. 12, no. 6, Jun. 2024, Art. no. 84, <https://doi.org/10.3390/technologies12060084>.
- [18] R. R. Elsharkawy, Khalid. F. A. Hussein, and A. E. Farahat, "Dual-Band (28/38 GHz) Compact MIMO Antenna System for Millimeter-Wave Applications," *Journal of Infrared, Millimeter, and Terahertz Waves*, vol. 44, no. 11, pp. 1016–1037, Dec. 2023, <https://doi.org/10.1007/s10762-023-00943-0>.
- [19] M. A. Aboulila, R. K. Hamad, A. I. Zaki, and M. H. Aly, "A Dual-Band (38 – 60 GHz) Antenna Designed for Millimeter Wave Wireless Communication Systems," in *2021 38th National Radio Science Conference (NRSC)*, Mansoura, Egypt, Jul. 2021, vol. 1, pp. 16–23, <https://doi.org/10.1109/NRSC52299.2021.9509830>.
- [20] M. V. Yadav, C. Kumar R, S. V. Yadav, T. Ali, and J. Anguera, "A Miniaturized Antenna for Millimeter-Wave 5G-II Band Communication," *Technologies*, vol. 12, no. 1, Jan. 2024, Art. no. 10, <https://doi.org/10.3390/technologies12010010>.
- [21] F. Y. Zulkifli, A. I. Wahdiyati, A. Zufar, N. Nurhayati, and E. Setijadi, "Super-Wideband Monopole Printed Antenna with Half-Elliptical-Shaped Patch," *Telecom*, vol. 5, no. 3, pp. 760–773, Sep. 2024, <https://doi.org/10.3390/telecom5030038>.
- [22] T. Tewary, S. Maity, S. Mukherjee, A. Roy, P. P. Sarkar, and S. Bhunia, "High gain miniaturized super-wideband microstrip patch antenna," *International Journal of Communication Systems*, vol. 35, no. 11, 2022, Art. no. e5181, <https://doi.org/10.1002/dac.5181>.

- 
- [23] S. Douhi *et al.*, "Design of a compact super wideband all-textile antenna for radio frequency energy harvesting and wearable devices," *Optical and Quantum Electronics*, vol. 55, no. 13, Oct. 2023, Art. no. 1189, <https://doi.org/10.1007/s11082-023-05498-x>.
- [24] S. Iriqat and S. Yenikaya, "Microstrip Patch Antenna Design With Enhanced Radiation Efficiency For 5G 60 GHz Millimeter-Wave Systems," *Uludağ Üniversitesi Mühendislik Fakültesi Dergisi*, vol. 29, no. 1, pp. 101–112, Apr. 2024, <https://doi.org/10.17482/uumfd.1366173>.
- [25] P. Merlin Teresa and G. Umamaheswari, "Compact Slotted Microstrip Antenna for 5G Applications Operating at 28 GHz," *IETE Journal of Research*, vol. 68, no. 5, pp. 3778–3785, Sep. 2022, <https://doi.org/10.1080/03772063.2020.1779620>.